

Influence of work environment on thermal state of electric mine motors

ROMAN KROK

*Institute of Electrical Engineering and Informatics,
Division of Electrical Machines and Electrical Engineering in Transport,
Silesian University of Technology,
Akademicka 10A, 44-100 Gliwice, Poland
e-mail: Roman.Krok@polsl.pl*

(Received: 10.05.2011, revised: ??2011)

Abstract: The paper presents a model for calculations of the temperature field in electric mine motors with a water cooled frame. That model was worked out with use of modified and improved thermal networks developed by the author for determining the temperature distributions in different types of ac machines. Thermal calculations for a selected type of 400 kW mining motor were performed with use of an original computer program. Their results were compared with those obtained from measurements. On the basis of the verified simulation results there was determined the influence of value changes of parameters characterising the work environment condition (ambient temperature, inlet temperature and cooling water discharge, degree of covering the casing with coal dust) on the mining motor thermal state.

Key words: electrical mining motors, thermal network method, exploitation of electric machines in coal mine undergrounds

1. Introduction

Thermal networks were originally (historically) used for determination of temperatures in electric machines. The first thermal diagrams of electromagnetic objects [1] contained mostly several nodes, which, in consequence, enabled calculation of only approximated values of mean temperatures of their basic elements.

The increase in the rated power of electric machines resulted in their more complex construction and development of cooling systems. Hence, the models in the form of thermal networks of electromagnetic objects have had to be continuously improved and modified. Due to numerous advantages, that method is still used for modelling the temperature distribution in electric machines [2-9].

The author created modified and improved thermal networks for calculations of the temperature field in ac machines containing developed networks of cooling ducts [10-12]. Tem-

perature distributions determined with their use are close to continuous distributions. Application of the optimal division of construction elements into difference elements ensures obtaining the high computation accuracy and much shorter time needed for carrying them out than in the case of using the finite element method. The created thermal networks enable determining two- and three- dimensional temperature distributions in electric machines when taking into account heating of medium streams flowing in the developed networks of cooling ducts – both in steady and transient thermal states. Such a way of modelling the temperature field in large ac machines has not been used so far.

The equivalent thermal diagram for a gas or fluid stream flowing in the cooling duct developed by the author is an important supplement of the equivalent thermal diagrams of electric machine constructional elements [11, 12]. It makes it possible to model the phenomena occurring both in constructional elements and cooling medium streams when taking into consideration the interaction between them. Using the developed thermal networks (containing from several hundred to several thousand nodes), one can determine the spatial temperature distributions in constructional elements and cooling medium streams. The results of thermal measurements for many types of mining motors [11, 12] and turbogenerators [10-12] confirmed the high accuracy of calculations carried out with use of the models developed.

The paper presents the temperature fields in mining motors with a developed network of cooling ducts, in which water or air flows, determined with use of the mentioned above method. Those models enable performing thermal simulation investigations of motors working under different environmental conditions in coal mine undergrounds. Those motors work at different: ambient temperature, temperature and cooling water discharge, and sometimes their casings are covered with coal dust. So, the right exploitation of a mining motor requires the knowledge of its thermal state under different conditions in coal mines. It is not possible to take thermal measurements of each type of a mining motor under all environmental conditions occurring in coal mines due to technical limitations and high costs. Investigations of the influence of value changes of parameters characterising the work environment conditions on the mining motor thermal state can only be performed with use of simulation methods.

2. Construction of electric mining motors with a cooled frame

In this section there are presented the construction and cooling system of mining motors with a water cooled frame on example of a 400 kW induction motor. The motor under consideration has a helical water duct (Figs. 1 and 2) in the frame. Water flows between two concentric tubes. The partition plates welded to the inner tube force the water flow along a helical path. The water flows in the frame from the side of a clutch (C) and flows out at the opposite side (O).

The inner air circulation in the motor (in Fig. 2 arrows denote directions of the air flow) is forced by a radial fan mounted on the shaft at the side of (O). The air is heated when flowing through axial ducts in the rotor core and is cooled when flowing through axial ducts in a water

cooler in the frame. The heat is carried away from the rotor active elements to the cooling water flowing in the frame by means of the air stream.

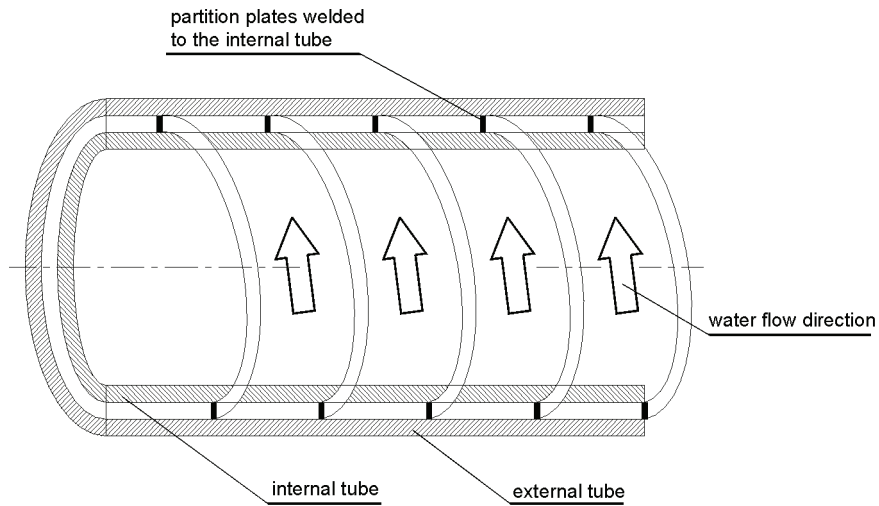


Fig. 1. Cooling water flow in a helical cooling duct in the mine motor frame

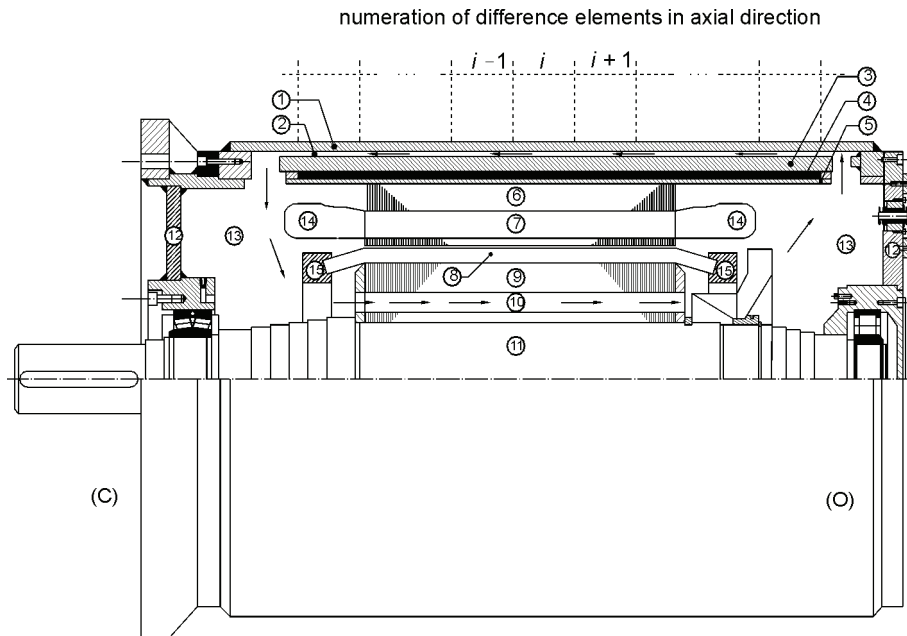


Fig. 2. Section of the 400 kW single speed mine motor with a water cooled frame including the introduced numeration of construction elements participating in the heat exchange

In the considered motor there were separated, and next numerated all constructional elements participating in the heat exchange:

- flame-proof enclosure (motor casing) – 1,
- axial air ventilation ducts in the frame – 2,
- external tube (Fig. 1) in the water cooler in the frame – 3,
- helical water duct in the frame – 4,
- internal tube in the water cooler in the frame – 5,
- stator core – 6,
- slot part of the stator winding – 7,
- bars of the rotor cage – 8,
- rotor core – 9,
- axial air ventilation ducts in the rotor core – 10,
- shaft – 11,
- bearing disks – 12,
- air inside the motor – 13,
- stator end windings – 14,
- rings shortening the rotor cage – 15.

3. Thermal network for the electric mining motor

In order to work out a thermal model, there were separated in the motor fifteen constructional elements (Fig. 2) participating in the heat exchange. Those elements together with the cooling ducts placed in them were divided in the axial direction (in which there exists the largest non-uniformity of the temperature distribution) into slices Δx wide. In that way in particular elements there were separated the difference elements, and next to each of them one thermal node was assigned (Fig. 3).

In the motor thermal model worked out there were taken into account:

- heat flow in particular constructional elements in axial and radial direction,
- different values of thermal conductivity of the stator and rotor cores in axial and radial direction,
- heat convection in water and air streams flowing through cooling ducts in the frame and rotor core,
- temperature changes in cooling media (water and air) streams along the duct length caused by the heat flow from the duct surface (or in opposite direction),
- power losses in the stator winding and rotor cage dependent on temperature,
- power losses in the stator core and bearings practically independent of temperature,
- carrying the heat away from constructional element surfaces in the motor interior to the air streams flowing around them and from the frame external surfaces to the environment.

The equivalent conductivities for the heat streams flowing due to conduction between the neighbouring difference elements (Fig. 3) were determined from the relationship:

$$G_{\lambda} = \frac{\lambda_x \cdot F}{\Delta x}, \quad (1)$$

where: λ_x – thermal conductivity of the material from which the constructional element in the x axis direction is made of, F – surface area of the wall separating the neighbouring difference elements.

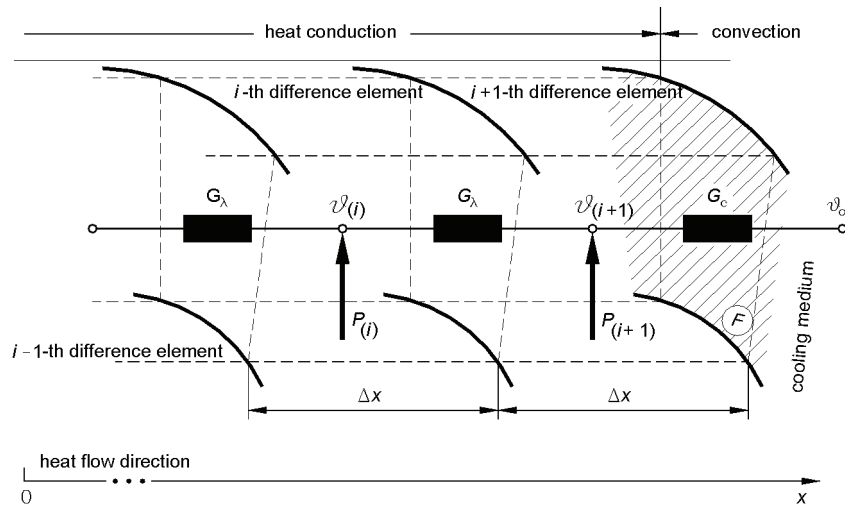


Fig. 3. Division of the exemplary motor construction part into elements in the axial direction and assigning the thermal network to it

The equivalent conductivities for the heat streams carried away from the walls of the difference elements (Fig. 3) to the cooling media flowing around them were determined from the relation:

$$G_c = \alpha_c \cdot F, \tag{2}$$

where: α_c – heat transfer coefficient, F – surface area of the element wall, from which the heat is transferred to the cooling medium flowing around it.

In the difference elements separated inside the stator and rotor windings (Fig. 3) there occur power losses dependent on temperature:

$$P_{(i)} = P_0 \cdot (1 + \alpha \cdot \vartheta_{(i)}), \quad P_0 = k_a \cdot j^2 \cdot \rho_0 \cdot V, \tag{3}$$

where: P_0 – power losses in the separated difference elements in the reference temperature (assumed to be equal to 0°C), α – temperature coefficient of resistance change of the material the windings are made of, $\vartheta_{(i)}$ – average temperature of the i -th difference element, k_a – additional loss coefficient, j – average current density in the winding, ρ_0 – resistivity of the material the winding is made of in the reference temperature, V – volume of the separated difference elements.

On the motor thermal diagram there are also power sources (Fig. 4) of discharges equal to the thermal powers convected by the streams of media flowing through the cooling ducts:

$$P_{m(i)} = \dot{m} c_p \vartheta_{m(i)}, \quad (4)$$

where: \dot{m} – stream of cooling medium mass, c_p – specific heat of the cooling medium per a unit mass at constant pressure (of water or air treated as an ideal gas), $\vartheta_{m(i)}$ – average medium temperature in the i -th difference element separated inside the duct.

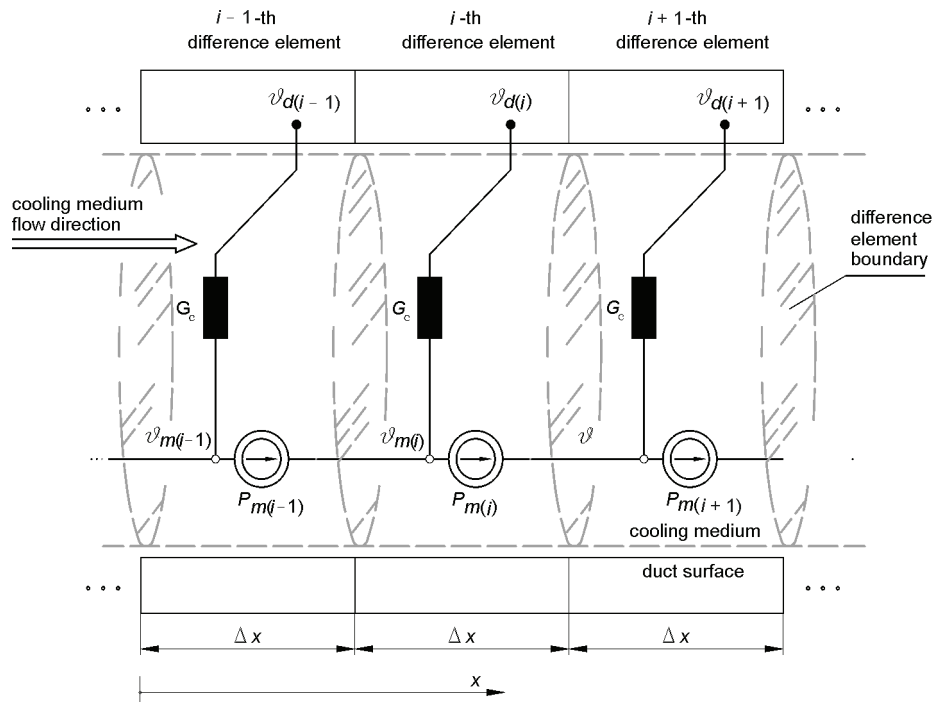


Fig. 4. Thermal network for a duct with flowing cooling medium stream

The thermal network for the considered 400 kW motor (Fig. 5) contains 158 nodes. It is the result of galvanic connection of the elementary equivalent diagrams assigned to the areas separated inside the constructional elements (of structure shown in Fig. 3) and the cooling ducts (of structure shown in Fig. 4).

As a result of applying the node potential method (here: node temperature method) to solving the thermal network, there was obtained a system of algebraic equations describing the temperature field in the considered motor in the form:

$$\mathbf{G} \cdot \vec{\vartheta} = \vec{P}, \quad (5)$$

where: \mathbf{G} – matrix of thermal conductivities, $\vec{\vartheta}$ – vector of node temperatures, \vec{P} – vector of thermal inputs.

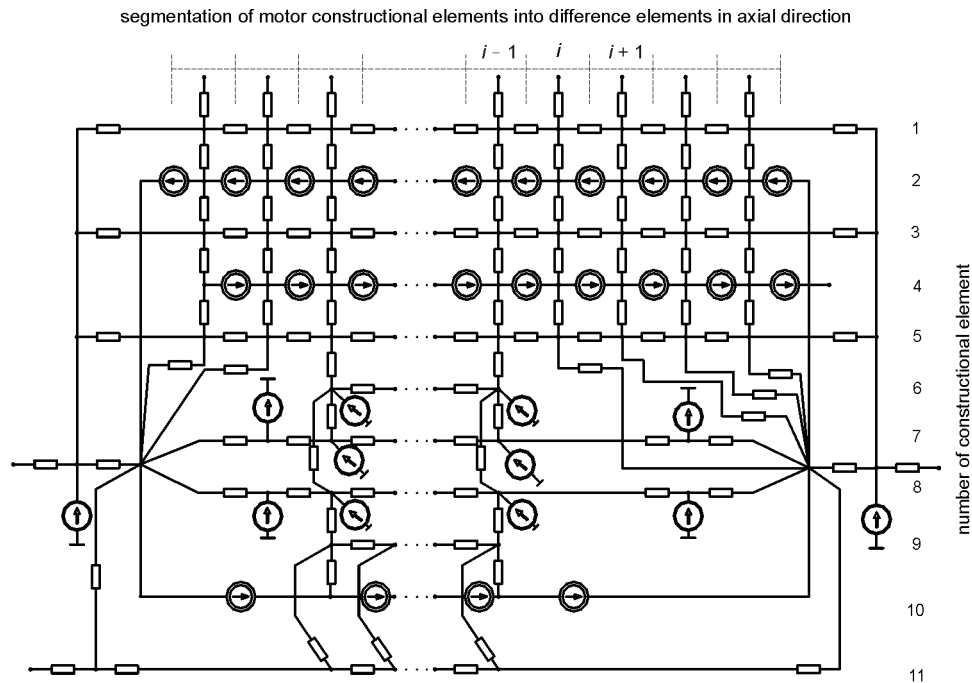


Fig. 5. Thermal network for the 400 kW electric mine motor

4. Measurement verification of thermal calculations of the electric mine motor

In order to determine the accuracy of representing the temperature by the worked out thermal network, there were taken thermal measurements of three 400 kW motors of the same type (denoted by symbols: „MOTOR 1”, „MOTOR 2” and „MOTOR 3”) under different cooling conditions and for different loads. The results obtained from measurements were compared with those from thermal calculations.

The rating of the mine motor of the considered type is as follows: $P_n = 400$ kW, $U_n=1000$ V, $I_n = 260$ A, $n_n = 1484$ rev/min.

The measurements of „MOTOR 1” and „MOTOR 2” were taken under the following cooling conditions: cooling water discharge - $Q_w = 13$ dm³/min, water temperature at the inlet to the frame - $\vartheta_w = 11.3^\circ\text{C}$, ambient temperature - $\vartheta_{ot} = 17.5^\circ\text{C}$. The motor was supplied with the rated voltage and its shaft power equaled 400 kW („MOTOR 1” and „MOTOR 2”) and 500 kW („MOTOR 2”). When taking measurements, the water circulation was open and the cold water temperature was relatively low and was equal to $\vartheta_w = 11.3^\circ\text{C}$. The average temperature of the stator winding was determined from the increase in resistance, and the maximum temperature was measured with a Pt 100 sensor built in the end windings at the side of (O). The results of measurements and thermal calculations of motors are given in Table 1.

Table 1. Calculation and thermal measurement results of mine motors "MOTOR 1" and "MOTOR 2"

Quantity	Rated load $P_n = 400 \text{ kW}$			Overload by 25% $P = 500 \text{ kW}$	
	Measurements		Calculations	Measurements MOTOR 2	Calculations
	MOTOR 1	MOTOR 2			
Stator winding average temperature	78.2°C	80.6°C	75.9°C	118.2°C	113.5°C
Stator winding maximum temperature	84.6°C	84.4°C	83.3°C	126.3°C	126.9°C

Under the considered operating conditions of the mine motors denoted by „MOTOR 1” and „MOTOR 2”, the maximal differences between the measured and calculated temperatures equal:

- 1.3 K for the maximum temperature of the stator winding,
- 4.7 K for the average temperature of the stator winding.

The average temperature of the stator winding is a weighted average of the temperatures of the thermal network nodes assigned to the separated difference elements in the windings.

There were also taken thermal measurements of the third mine motor of the considered type ("MOTOR 3") for the cooling water closed circulation for which the steady inlet temperature was significantly higher than that from the previous measurement and equaled $\vartheta_w = 30.0^\circ\text{C}$. The values of the other parameters characterising the mine motor cooling conditions were as follows: cooling water discharge – $Q_w = 15 \text{ dm}^3/\text{min}$, ambient temperature – $\vartheta_{ot} = 24.0^\circ\text{C}$. During investigations the motor was supplied with the rated voltage and loaded with the rated mechanical power of 400 kW. The calculation and thermal measurement results of that motor are given in Table 2.

Table 2. Calculation and thermal measurement results of the mine motor „MOTOR 3”

Quantity	Rated load $P_n = 400 \text{ kW}$	
	Measurements	Calculations
Stator winding average temperature	97.0°C	93.2°C
Stator winding maximum temperature	103.9°C	100.6°C
Cooling water outlet temperature	36.5°C	38.5°C

Under the considered operating conditions of the mine motor denoted by „MOTOR 3”, the differences between the measured and calculated temperatures equal:

- 3.3 K for the maximum temperature of the stator winding,
- 3.8 K for the average temperature of the stator winding,
- 2.0 K for the cooling water temperature at the outlet from the frame.

The maximal difference between the calculated and measured temperature in the motor constructional elements for different loads and under different cooling conditions is equal to 4.7 K. The worked out thermal model also represents very well the cooling water temperature value at the outlet from the frame (with the error not bigger than 2.0 K), and, in consequence, the value of the thermal power carried out from the motor (dependent on the cooling water temperature difference at the inlet and outlet from the frame) by the cooling water stream. Taking into account the spread of the temperature values measured in different motors in the same elements and under the same operating conditions, the obtained calculation accuracy should be recognized to be satisfying.

5. Investigations of the electric mine motor thermal state under different operating conditions occurring in coal mine undergrounds

Using the thermal network worked out for the 400 kW mine motor, simulation investigations aiming at determination of the influence of value change of parameters characterising the work environment condition on the motor thermal state were performed.

The calculated axial temperature distributions in the stator winding and the cooling water stream in the frame under the following cooling conditions: $\vartheta_w = 30^\circ\text{C}$, $\vartheta_{ot} = 25^\circ\text{C}$, are presented for:

- the motor loaded with the rated mechanical power $P_n = 400$ kW and for the rated cooling water discharge $Q_{wn} = 15$ dm³/min (Fig. 6),
- the motor loaded with the rated mechanical power $P_n = 400$ kW and the emergency decrease in the cooling water discharge to $Q_w = 10$ dm³/min (Fig. 7),
- simultaneous overloading of the motor by 20% ($P = 480$ kW) and the emergency decrease in the cooling water discharge to $Q_w = 10$ dm³/min (Fig. 8).

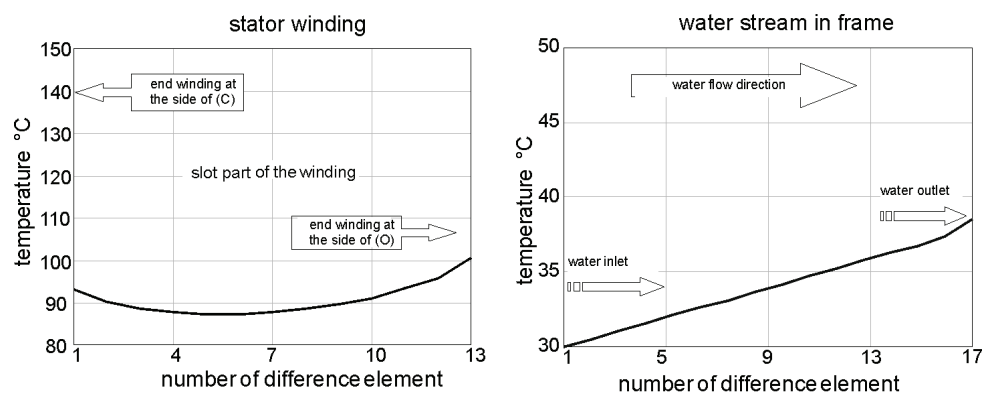


Fig. 6. Axial temperature distributions in mine motor stator loaded with rated power $P_n = 400$ kW and for cooling water discharge $Q_w = 15$ dm³/min

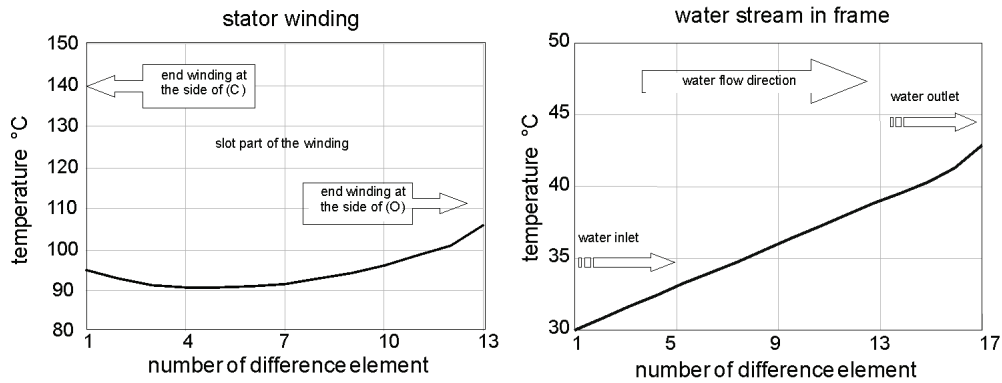


Fig. 7. Axial temperature distributions in mine motor stator loaded with rated power $P_n = 400$ kW and for cooling water discharge $Q_w = 10$ dm³/min

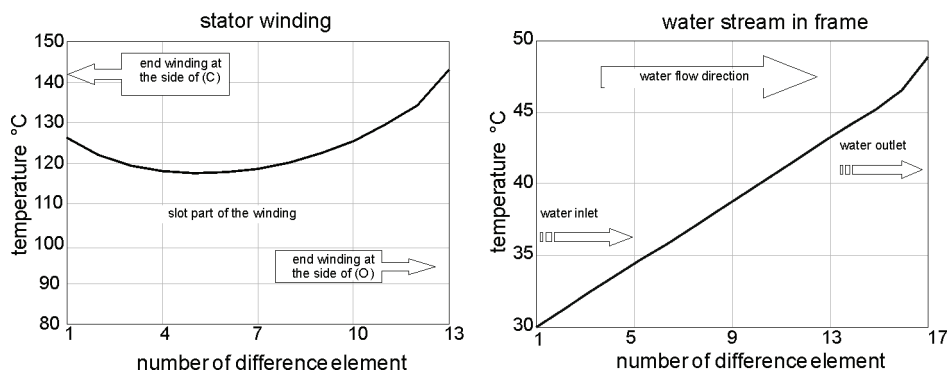


Fig. 8. Axial temperature distributions in mine motor stator for motor overloaded by 20% ($P = 480$ kW) and for cooling water discharge $Q_w = 10$ dm³/min

Increase in the maximum temperature of the motor stator winding above the permissible value results in shortening the insulation life, and in the extreme case in its damage. The proper exploitation of motors working under different environmental conditions existing in coal mine undergrounds requires, first of all, keeping the maximum temperature of the stator winding at the level not exceeding the permissible value resulting from the class of insulation heat-resistance.

Using the thermal network worked out for the 400 kW mine motor, there were calculated the dependencies of the stator winding maximum temperature on:

- inlet cooling water temperature (Fig. 9),
- ambient temperature (Fig. 10),
- cooling water discharge (Fig. 11),
- coefficient of heat penetration from the casing surface to the environment dependent on the degree of covering the motor with coal dust (Fig. 12).

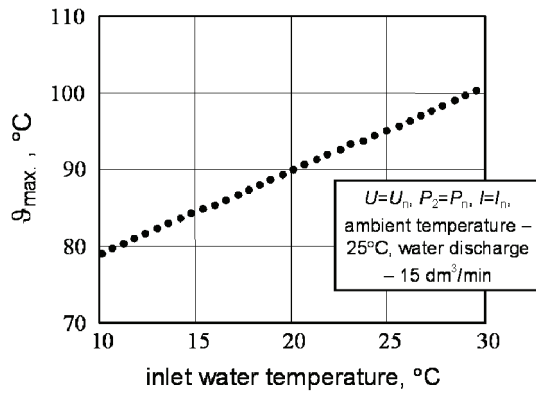


Fig. 9. Dependence between the stator winding maximum temperature and the temperature of cooling water at the inlet to the frame

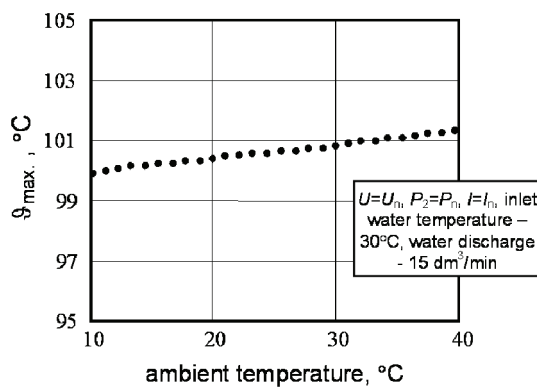


Fig. 10. Dependence between the stator winding maximum and ambient temperature

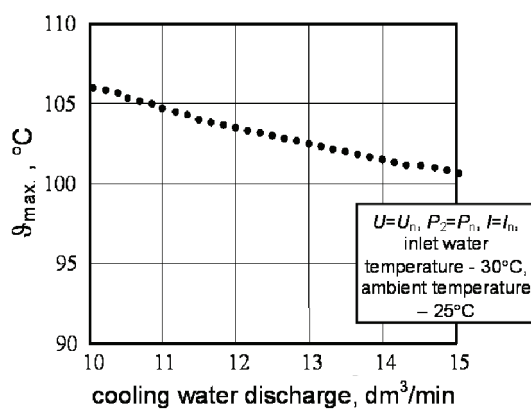


Fig. 11. Dependence between the stator winding maximum temperature and the cooling water discharge

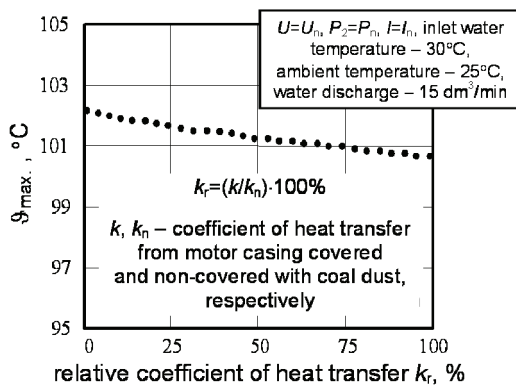


Fig. 12. Dependence between the stator winding maximum temperature and the relative coefficient of heat transfer from the casing external surface

From the obtained thermal simulation results of the considered mine motor working under different environmental conditions, the following conclusions can be drawn:

- increase in the temperature of cooling water flowing into the frame (Fig. 9) results in growth, by the same value approximately, the stator winding maximum temperature,
- change of the ambient temperature within the very wide range, from 10 to 40°C (Fig. 10) causes very small (not exceeding 2.5 K) change of the stator winding maximum temperature value (practically almost the whole thermal power produced in active motor elements is carried away to the water cooler in the frame, in consequence, change of the ambient temperature does not influence essentially the temperature of elements inside the frame),
- cooling water discharge (Fig. 11) influences essentially the motor thermal state – e.g. decrease in the cooling water discharge from 15 to 10 dm³/min results in increase in the stator winding maximum temperature by about 6 K,
- covering the motor with coal dust (Fig. 12), resulting in decrease of the equivalent coefficient of heat penetration from the casing surface to the environment, does not cause the essential change of the stator winding maximum temperature value (that temperature after complete covering the motor, making carrying away of the heat to the surroundings impossible, increases only by 2 K).

There were also carried out comparative thermal calculations of the mine motor overloaded by 20% ($P = 480$ kW) for emergency decrease in the cooling water discharge to 10 dm³/min and the rated cooling water discharge equal to 15 dm³/min. The maximum temperatures of the basic constructional nodes of the motor and of the water at the cooler outlet are given in Table 3.

For the mine motor overloaded by 20% at the cooling water discharge decreased to 10 dm³/h and simultaneous increase in the inlet water temperature to 30°C, the maximum increase in the stator winding temperature equals 143.1°C and is smaller by 36.9°C than the permissible one for the used insulation made in the H heat-resistance class (180°C). The outlet temperature of the cooling water is equal to 48.9°C, so it is significantly smaller than the water boiling point. Then, the motor can work under the considered emergency operating condition of the water cooler. However, one should remember that increase in the stator winding insula-

tion temperature caused by decrease in discharge or increase in temperature of the inlet cooling water results in decrease of insulation life.

Table 3. Thermal calculation results of the mine motor overloaded by 20% ($P = 480$ kW) for different discharge and inlet temperature of cooling water in the ambient temperature 25°C

Water discharge dm^3/min	Water inlet temperature $^{\circ}\text{C}$	Maximum temperature $^{\circ}\text{C}$			
		stator winding	rotor cage	casing surface	cooling water
15	10	111.5	178.7	61.9	22.2
15	20	123.1	193.0	71.0	32.3
15	30	134.6	207.3	80.1	42.5
10	10	119.9	189.7	69.8	28.6
10	20	131.5	204.0	79.0	38.7
10	30	143.1	218.4	88.3	48.9

6. Concluding remarks

1. The worked out thermal networks enable performing thermal simulations of large electric mine motors working under different environmental conditions in coal mine undergrounds. They concern thermal hazards of motors resulting from the change of exploiting conditions as well as work safety in coal mines being in danger of explosion for which keeping the casing temperature at the appropriate low level is essential. The temperature distributions determined in all constructional elements as well as in flowing streams of cooling media allow estimating the thermal state of these motors accurately.
2. The developed computation programs are also applied to computer aided design of electric mine motors. The spatial temperature distributions in a motor calculated with use of them allow improving the motor construction already at the stage of design. Simulation investigations enable also determining the permissible range of value changes of parameters characterising the work environment condition for which the danger of motor thermal damage does not exist as well as the motor life given by a manufacturer is kept.
3. The thermal networks for worked out electric mine motors can also be a supporting tool for works connected with design and setting of thermal protections when taking into account the environmental conditions occurring in a coal mine.

References

- [1] Hak J., *Die inneren axialen Wärmewiderstände einer elektrischen Maschine*. Archiv. für Elektrotechnik Heft 1: 58-76 (1957).
- [2] Kalander G., *Temperature simulation of a 15 kW induction machine operating at variable speed*. International Conference on Electrical Machines, Manchester, UK (1992).

- [3] Rioul M., *Development of thermohydraulic modelling for the determination of hot spots in the bars and the slot thermal image for the stator 900 MW turbogenerators*. Proceedings of ICEM'94, Paris, France, pp. 437-441 (1994).
- [4] Elleuch M., Poloujadoff M., *A contribution to the modelling of three phase transformers using reluctances*. IEEE Transactions on Magnetics 32: 335-343 (1996).
- [5] Mukosiej J., *Universal program for thermal calculation of electric machines by the method of equivalent thermal networks (ETN)*. Proceedings of ICEM'96, Vigo, Spain: 377-381 (1996).
- [6] Tylavsky D.J., Qing He, Jennie Si et al., *Transformer top-oil temperature modeling and simulation*. IEEE Transactions on Industry Applications 36(5): 1219-1225 (2000).
- [7] Swift G., Molinski T.S., Lehn W., *A fundamental approach to transformer thermal modeling – Part I: Theory and equivalent circuit*. IEEE Transactions on Power Delivery 16: 171-175 (2001).
- [8] Radakovic Z., Maksimovic S., *Non-stationary thermal model of indoor transformer stations*. Electrical Engineering 84 (2002).
- [9] Gurazdowski D., Zawilak J., *Rozkład temperatury w pręcie uzwojenia stojana turbogeneratora. (Temperature distribution in the turbogenerator stator winding bar)* Zeszyty Problemowe – Maszyn Elektryczne Komet 75: 177-184 (2006).
- [10] Krok R., Miksiewicz R., *Application of thermal resistance network for the analysis of thermal fields in turbogenerator rotors with director and intermediate cooling of windings*. Proceedings of ICEM'96, Vigo, Spain 1996.
- [11] Krok R., *Sieci cieplne w modelowaniu pola temperatury w maszynach elektrycznych prądu przemiennego. (Thermal networks for modelling the temperature field in AC electric machines)* Wydawnictwo Politechniki Śląskiej, Gliwice, Poland (2010).
- [12] Krok R., *Sieci cieplne w modelowaniu pola temperatury w maszynach elektrycznych i transformatorach. (Thermal networks for modeling the temperature field in electric machines and transformers)* Przegląd Elektrotechniczny 10: 318-323 (2010).